

F-actin binding is essential for coronin 1B function in vivo

Liang Cai¹, Alexander M. Makhov² and James E. Bear^{1,*}

¹Lineberger Comprehensive Cancer Center and Department of Cell & Developmental Biology, and ²Department of Microbiology & Immunology, University of North Carolina at Chapel Hill, Chapel Hill, North Carolina, 27599-7295, USA

*Author for correspondence (e-mail: jbear@email.unc.edu)

Accepted 2 April 2007

Journal of Cell Science 120, 1779-1790 Published by The Company of Biologists 2007
doi:10.1242/jcs.007641

Summary

Coronins are conserved F-actin binding proteins that have been implicated in a variety of processes including fibroblast migration, phagocytosis, and chemotaxis. Recent data from our lab indicate that coronin 1B coordinates Arp2/3-dependent actin filament nucleation and cofilin-mediated filament turnover at the leading edge of migrating fibroblasts. Analysis of coronin function has been hampered by the lack of a clear understanding of how coronin interacts with F-actin. Here, we identify a surface-exposed conserved arginine residue at position 30 (R30), which is crucial for coronin 1B binding to F-actin both in vitro and in vivo. Using actin co-sedimentation, we demonstrate that coronin 1B binds with high affinity to ATP/ADP- P_i -F-actin (170 nM) and with 47-fold lower affinity to ADP-F-actin (8 μ M). In contrast to a previous study, we find no evidence for

enhanced cofilin binding to F-actin in the presence of either coronin 1B or coronin 1A. Instead, we find that coronin 1B protects actin filaments from cofilin-induced depolymerization. Consistent with an important role for interactions between coronin 1B and F-actin in vivo, an R30D coronin mutant that does not bind F-actin localizes inefficiently to the leading edge. Furthermore, our analysis indicates that F-actin binding is absolutely required for coronin 1B to exert its effects on whole-cell motility and lamellipodial dynamics.

Supplementary material available online at
<http://jcs.biologists.org/cgi/content/full/120/10/1779/DC1>

Key words: Coronin, Actin, Cofilin, Arp2/3, FRAP

Introduction

The dynamic reorganization of the actin cytoskeleton is a crucial component in nearly all aspects of cell motility (Pollard and Borisy, 2003). Actin polymerization itself is thought to provide the driving force during leading edge protrusion. Dynamic actin reorganization also plays an important role in other processes such as host-pathogen interactions and endocytosis (Bear et al., 2001; Engqvist-Goldstein and Drubin, 2003). The molecular mechanisms of actin assembly and dynamics have been the target of intense study for decades. A host of cellular proteins control the nucleation, growth, organization and disassembly of actin filaments. Coronins are F-actin-binding proteins that are highly conserved across species and regulate a number of motility processes (Utrecht and Bear, 2006). However, the mechanism by which coronins affect cell motility has not been fully elucidated.

Functional studies from multiple species indicate that coronins play important roles in many processes involving actin dynamics. Coronin was originally identified in *Dictyostelium* as an F-actin-binding protein that is enriched at the leading edge and at phagocytic cup structures (de Hostos et al., 1991). *Dictyostelium* mutants lacking coronin have defects in cell migration, cytokinesis and phagocytosis (de Hostos et al., 1993; Maniak et al., 1995). Yeast coronin crosslinks actin filaments and microtubules, and overexpression induces the formation of abnormal actin loop

structures (Goode et al., 1999; Humphries et al., 2002). Mammals have six coronin genes that are divided into three subclasses (Utrecht and Bear, 2006). Coronin 1B is an ubiquitously expressed isoform that localizes to the leading edge of migrating fibroblasts (Cai et al., 2005). Depletion of coronin 1B influences lamellipodial protrusion and whole-cell motility by altering the actin dynamics and architecture at the leading edge (Cai et al., 2007). Coronin 1B was also identified as an important factor for neurite outgrowth in a neuronal regeneration model (Di Giovanni et al., 2005). Deletion of coronin 1A, a hematopoietic specific isoform, in mice leads to severe defects in lymphocyte homeostasis and T-cell chemotaxis (Fogor et al., 2006).

One mechanism by which coronins exert an effect on motility is through the inhibition of the Arp2/3 complex. This observation was originally made in yeast where coronin interacts with the Arp2/3 complex in vivo and in vitro, and directly inhibits actin nucleation mediated by the Arp2/3 complex (Humphries et al., 2002). Human coronin 1B also interacts with the Arp2/3 complex in vivo and specifically inhibits Arp2/3-complex-induced actin nucleation in vitro (Cai et al., 2005; Cai et al., 2007). The interaction between coronin 1B and the Arp2/3 complex is regulated by phosphorylation of the serine residue 2 (Ser2) via PKC (Cai et al., 2005). Ser2 phosphorylation also controls the interaction of coronin 1A with the Arp2/3 complex (Fogor et al., 2006).

Another important mechanism by which coronins affect motility is through the regulation of ADF/cofilin proteins (hereafter referred to as cofilin). Cofilin promotes the disassembly of actin filaments primarily through severing, although other evidence suggests that these proteins may also promote enhanced pointed end depolymerization (Bamburg, 1999). Coronin 1B targets the cofilin-activating phosphatase slingshot-1L to the leading edge and, thus, indirectly regulates cofilin activity *in vivo* (Cai et al., 2007). In addition to regulating slingshot-1L targeting, coronin 1B can also be dephosphorylated on Ser2 by slingshot-1L. Genetic studies in yeast have shown that the combination of coronin gene deletion with a mutation in the cofilin gene causes lethality, suggesting a functional link between coronin and cofilin in this organism (Goode et al., 1999). Recent work using reconstituted *Listeria* actin comet tails as a model system for actin assembly/disassembly identified coronin 1A as a factor that enhances cofilin-dependent actin depolymerization (Briehner et al., 2006). The authors of this study postulated that coronin 1A promotes cofilin severing activity by enhancing its binding to the sides of actin filaments.

Although coronin was originally identified by its ability to

bind actin filaments, the precise actin-binding site has yet to be unequivocally identified. In fact, actin-binding sites have been mapped to nearly every part of the protein (Uetrecht and Bear, 2006). The recent crystal structure of coronin 1A demonstrated that the majority of the protein participates in a seven-bladed β -propeller (Appleton et al., 2006). This structure includes two cryptic blades that flank the five known WD40 repeats and a C-terminal extension that folds tightly along the bottom of the β -propeller. Many of the earlier attempts to map the F-actin-binding site of coronin used truncation mutants that contained fragments of this compact structure (Gatfield et al., 2005; Liu et al., 2006; Mishima and Nishida, 1999; Oku et al., 2003; Spoerl et al., 2002). These fragments may not adopt stable or physiological conformations and the results of these studies must be confirmed using mutations in the full-length protein (Appleton et al., 2006). Since no clear consensus about the F-actin-binding site has been established, the requirement for the F-actin-binding activity of coronin *in vivo* has not yet been tested. The work presented here describes the identification of a conserved residue (R30) that is crucial for binding to actin filaments, and establishes the importance of F-actin-binding activity for coronin 1B function *in vivo*.

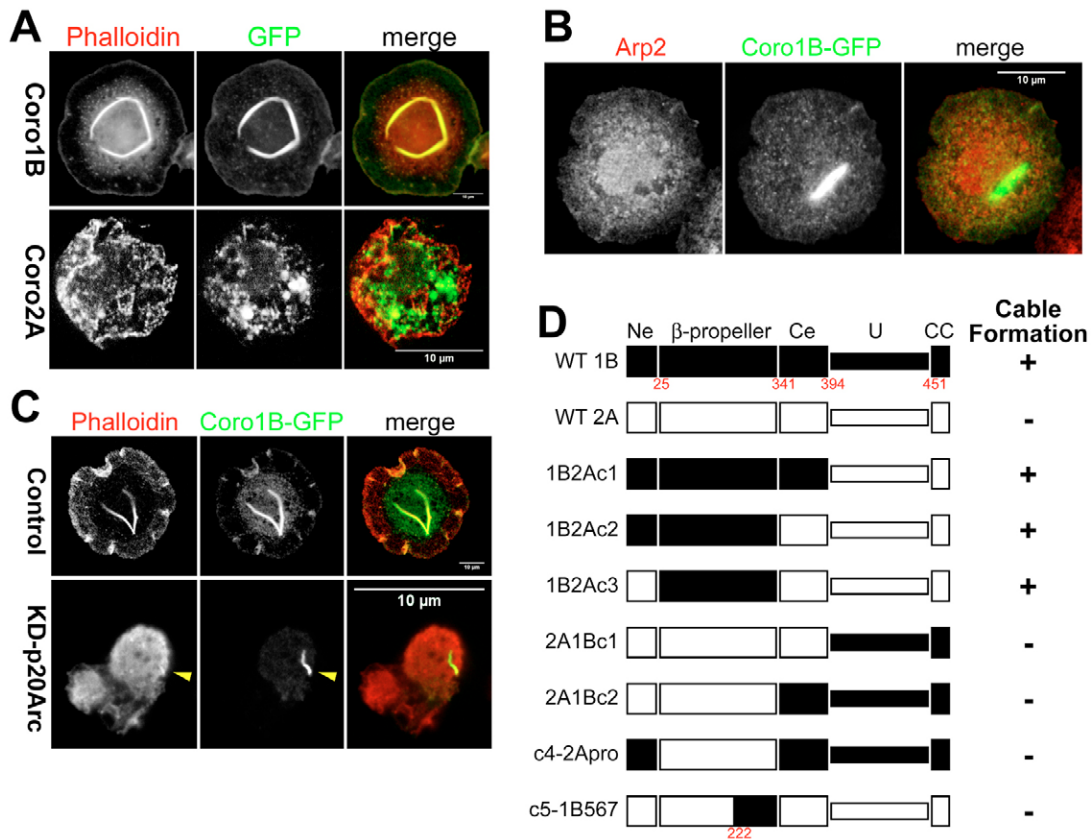


Fig. 1. Coronin 1B induces F-actin cables in *Drosophila* S2 cells independently of the Arp2/3 complex. (A) S2 cells were transfected with GFP-tagged coronin 1B or coronin 2A expression constructs, plated on ConA-treated coverslips, and stained for F-actin using phalloidin. (B) S2 cells transfected with GFP-tagged coronin 1B expression constructs were immunostained for Arp2, a subunit of the Arp2/3 complex. (C) Endogenous *Drosophila* p20Arc was depleted by siRNA for 7 days. S2 cells were transfected with coronin 1B expression constructs and stained with phalloidin. Arrowheads show a colocalization of F-actin and coronin 1B in p20Arc depleted S2 cells. (D) Diagram of coronin-1B–coronin-2A chimeras showing cable-formation ability of each construct. Fragments from coronin 1B are in black, and fragments from coronin 2A are in white. Red numbers indicate the start position of each region according to amino acid sequence of coronin 1B. Corresponding coronin 2A regions were chosen by sequence alignment using ClustalX 1.83.

Results

Ectopic expression of coronin 1B in *Drosophila* S2 cells induces F-actin cables

While generating a stable *Drosophila* S2 cell line to produce recombinant human coronin 1B, we observed that ectopic expression of this protein induced the formation of F-actin-containing cable-like structures. These actin cables stain with phalloidin and contain most of the ectopic coronin 1B (Fig. 1A). Previous studies of yeast coronin showed that overexpression of this protein induced the formation of Arp2/3-containing aberrant F-actin loop structures (Humphries et al., 2002). In the case of ectopic expression of coronin 1B in S2 cells, we cannot detect Arp2/3 complex in these coronin-1B-actin cables (Fig. 1B). To test whether the coronin-1B-induced actin cables in S2 cells require the presence of functional Arp2/3 complex, we depleted the p20Arc subunit of the Arp2/3 complex in S2 cells using small interfering RNA (siRNA) of an established sequence (Rogers et al., 2003). Depletion of p20Arc blocks the spreading of S2 cells on concanavalin A (ConA)-coated surfaces as reported previously, but does not appear to inhibit the formation of coronin-1B-containing actin cables (Fig. 1C, yellow arrowhead). Thus, ectopic coronin 1B expression in insect cells induces the formation of heavily bundled actin structures without a strict requirement for wild-type levels of Arp2/3. We postulate that the ability to form these cables is a reflection of the F-actin binding and/or bundling activity of coronin 1B in vivo.

Interestingly, ectopic expression of another mammalian coronin, coronin 2A, does not induce actin cables (Fig. 1A). Consistent with this, coronin 2A appears to interact weakly with F-actin in vitro (our unpublished observation). We exploited this difference between coronin 1B and coronin 2A to identify the part of coronin 1B that confers the ability to induce actin cable formation and thus F-actin binding and/or bundling. Based on the recently published coronin 1A structure (Appleton et al., 2006) and homology modeling (supplementary material Fig. S1), we designed a series of coronin-1B–coronin-2A chimeras to map the region on coronin 1B that is responsible for actin cable formation. We find that the β -propeller region of coronin 1B is both necessary and sufficient to induce the formation of actin cables (Fig. 1D). Using the chimera c5-1B567, we further narrowed our search for the actin-cable-forming region to the first four blades of the β -propeller of coronin 1B.

Identification of a crucial F-actin-binding residue on the surface of the β -propeller

Using our structural model of coronin 1B, we systematically mutated charged, surface-exposed residues that differ between coronin 1B and 2A in the first four blades of the β -propeller. We used both alanine substitutions and charge-reversal mutations, and tested the ability of these mutants to induce actin cables in S2 cells (Fig. 2A,B). Mutation of arginine at position 30 to alanine (R30A) attenuated the ability of coronin 1B to induce cables, whereas the charge-reversal mutation of this residue (R30D) completely abolished cable formation. According to our homology model, R30 is a surface-exposed residue, has no predicted side-chain interactions with surrounding residues, and

directly faces the lysine residue at position 73 (K73) (Fig. 2D and 2E). A charge-reversal mutation of K73 also greatly reduced the formation of actin cables, supporting the importance of a charged patch containing R30 in actin-cable formation. Based on multiple sequence alignments of coronin proteins from different species, we find that R30 is a highly conserved charged residue that is invariably flanked by two hydrophobic residues isoleucine/leucine and valine/leucine (Fig. 2C).

R30 is essential for coronin 1B binding to F-actin in vitro

To directly test the role of R30 in the binding of coronin 1B to F-actin, we first characterized the F-actin-binding properties of wild-type coronin 1B by using high-speed actin co-sedimentation assays. We purified full-length recombinant coronin 1B to >99% purity using a mammalian protein expression system (supplementary material Fig. S2). Recombinant coronin 1B binds robustly to F-actin in vitro (Fig. 3A). The stoichiometry of coronin 1B binding to F-actin (~2.6:1) exceeds a 1:1 ratio, an effect probably due to oligomerization of coronin 1B via its coiled-coil domain. We also examined the salt-sensitivity of the coronin-1B–F-actin interaction (Fig. 3B). This interaction occurs at physiological salt concentrations (100 mM KCl) and lower, but is reduced under high-salt conditions (150 mM KCl).

In order to test whether the nucleotide state of the actin filaments regulates coronin 1B binding, we polymerized filaments from ADP-G-actin or ATP-G-actin and repeated the co-sedimentation assays (supplementary material Fig. S3). After polymerization, bound ATP on individual actin subunits is hydrolyzed to ADP- P_i at a rate of 0.3 second⁻¹, followed by the slow release of inorganic phosphate (P_i) at a rate of 0.002 second⁻¹ to form ADP-F-actin (Pollard et al., 2000). As a result of this rate differential of 150, newly polymerized filaments generated from ATP-G-actin are composed mainly of ATP- and ADP- P_i -F-actin. Actin filaments assembled from ADP-G-actin are composed entirely of ADP-F-actin. Coronin 1B binds preferentially to filaments prepared from ATP-G-actin over filaments prepared from ADP-G-actin (Fig. 3C–E). To calculate the affinity of coronin 1B binding to F-actin, we used an established supernatant-depletion method (Bryce et al., 2005). Bound coronin 1B was calculated from the amount depleted from the supernatant as detected by immunoblotting and densitometry. To facilitate the affinity measurements and avoid the complicating factor of oligomerization, a sub-stoichiometric amount of coronin 1B (0.1 μ M) was used in these reactions. Our results show that coronin 1B binds to ATP/ADP- P_i -F-actin with an affinity of 170 nM, and to ADP F-actin with an affinity of 8 μ M. Thus, coronin 1B binds to actin filaments containing ATP/ADP- P_i approximately 47 times stronger than actin filaments containing ADP.

To test whether the R30D mutant binds to F-actin, we prepared a recombinant version of this protein and performed co-sedimentation assays. The R30D mutant displays extremely poor F-actin-binding capability in vitro (Fig. 3F,G). The small amount of R30D mutant protein that pellets with actin filaments may reflect residual low-affinity F-actin binding or non-specific entrapment of the protein in the F-actin pellet. To exclude the possibility that the R30D mutation leads to protein misfolding, we compared wild-type coronin 1B with the R30D mutant using both limited

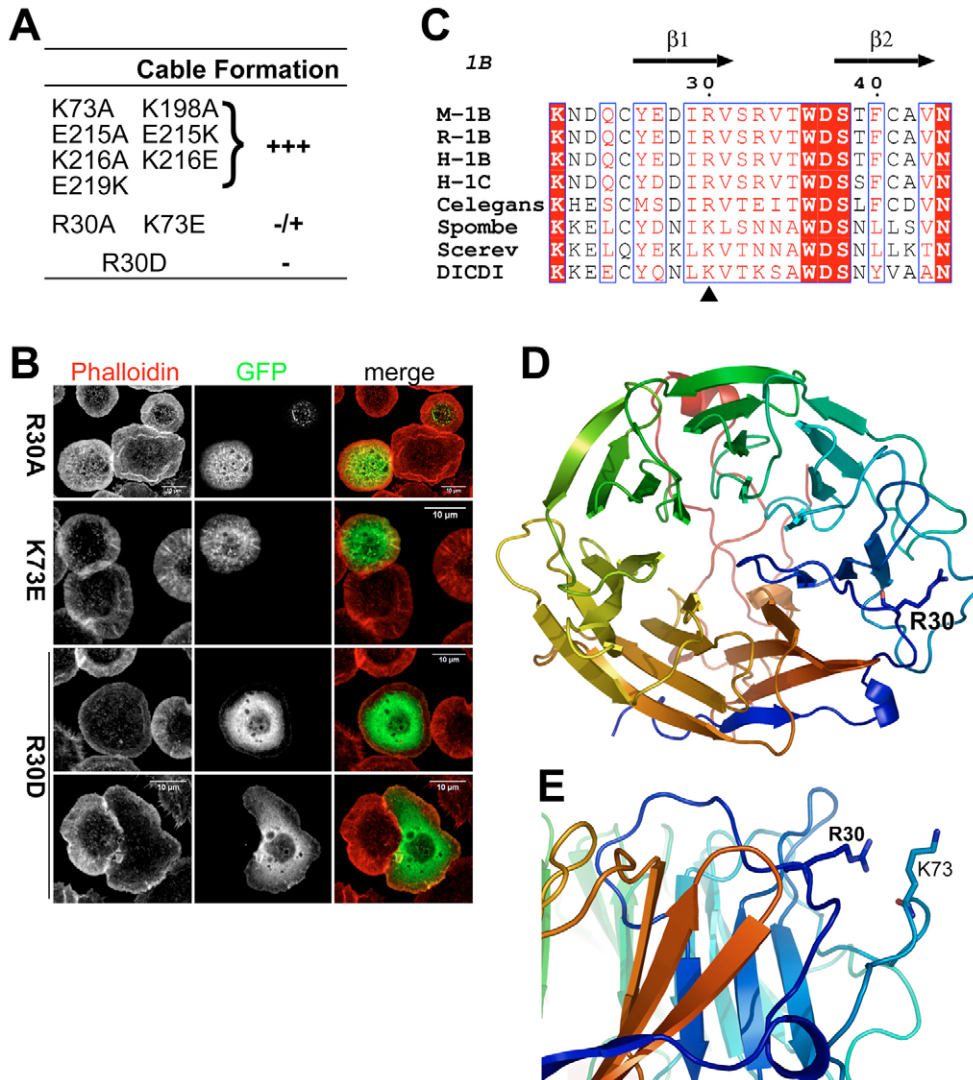


Fig. 2. A conserved surface-exposed arginine residue, R30, in coronin 1B is responsible for actin-cable formation. (A) Charged, surface-exposed residues within the first and fourth blades of the coronin 1B β -propeller were mutated to alanine or an amino acid with an opposite charge (i.e. R \rightarrow D). Cable-formation capability was scored as follows: +++, >99% of transfected cells contain GFP-positive actin cables; +/-, <50% of transfected cells contain actin cables, the rest have phalloidin-positive, small GFP aggregates; -, <1% of transfected cells contain phalloidin-positive GFP aggregates, the majority show high levels of cytoplasmic GFP. (B) S2 cells were transfected with the indicated GFP-tagged coronin 1B mutants and stained with phalloidin. (C) Multiple sequence alignment shows that R30 is a highly conserved charged residue in coronins, and locates between the first and second β -sheet in the propeller structure. M-1B, *Mus musculus* coronin 1B (gi:12229769); R-1B, *Rattus norvegicus* coronin 1B (gi:12229732); H-1B, *Homo sapiens* coronin 1B (gi:21263481); H-1C, *Homo sapiens* coronin 1C (gi:7656991); Celegans, *Caenorhabditis elegans* coronin (gi:3121874); Spombe, *Schizosaccharomyces pombe* coronin (gi:3121869); Scerev, *Saccharomyces cerevisiae* coronin (gi:3121873); DICDI, *Dictyostelium discoideum* coronin (gi:116950). The multiple alignment was generated using ClustalX 1.83 and illustrated using ESPRIPT. (D) Top view of coronin 1B homology model. N-terminus is blue, C terminus is red. The side chain of R30 is presented in stick form. The homology model was generated in InsightII-2005 using HOMOLOGY model, and evaluated by Profile_3D function (see supplementary material Fig. S1). Illustration was generated using Pymol (<http://www.pymol.org>). (E) Side view of coronin 1B structural model showing the positions of R30 and K73.

proteolysis and circular dichroism analysis (supplementary material Fig. S4). Results show that the two proteins have indistinguishable protease K digestion patterns and similar molar ellipticity profiles, indicating the R30D mutation does not grossly affect protein structure. To further confirm this result, we tested the ability of the R30D mutant to oligomerize with wild-type coronin 1B to be phosphorylated and dephosphorylated, and to bind directly to purified Arp2/3

complex in vitro (Fig. 4A-D, supplementary material Fig. S6). In all cases, the R30D mutant behaves identically to the wild-type protein, indicating that this mutation selectively affects F-actin binding but not other molecular interactions. Interestingly, the co-immunoprecipitation between coronin 1B and the Arp2/3 complex from cell lysates is reduced by the R30D mutation, suggesting that F-actin binding increases the coronin 1B-Arp2/3 interaction in vivo (Fig. 4E).

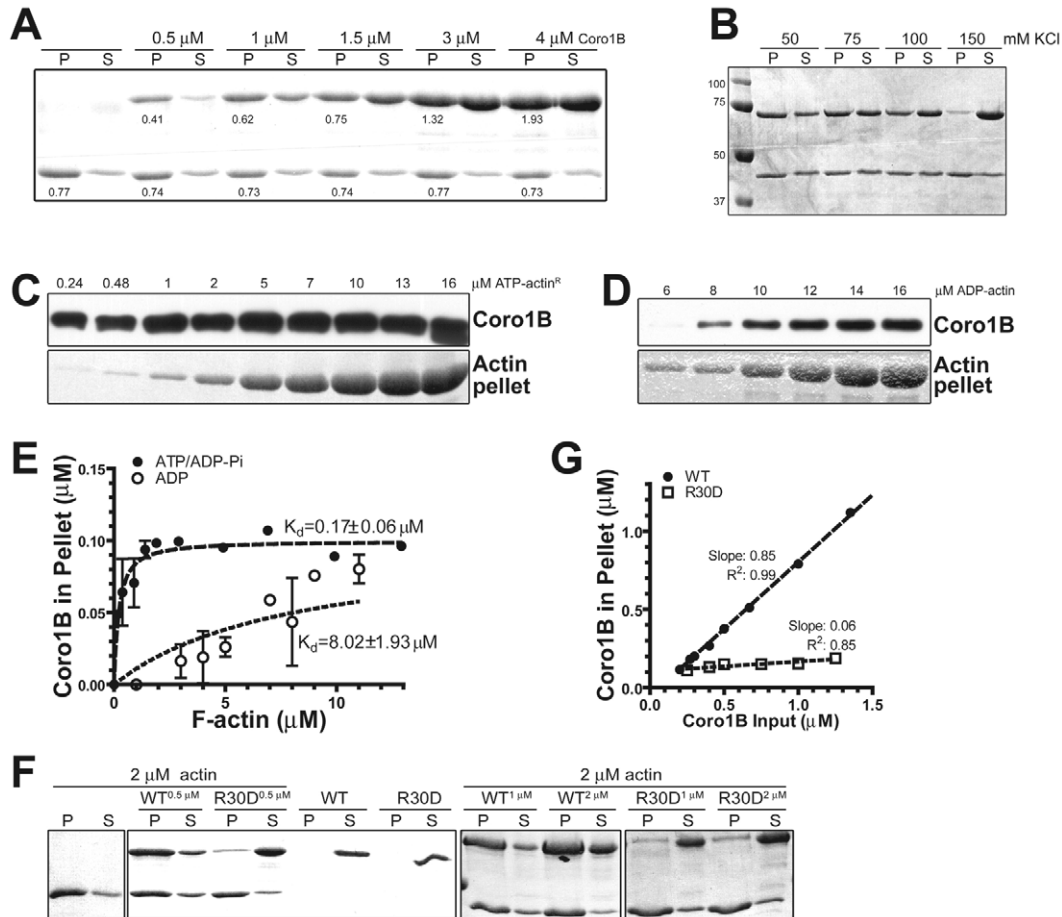


Fig. 3. Coronin 1B preferentially binds to ATP/ADP- P_i -F-actin and mutation of R30 abolishes binding. (A) Representative Coomassie-Blue-stained gel showing the near-saturation binding of coronin 1B to ATP/ADP- P_i -F-actin (1 μ M total actin). Upper band, coronin 1B; lower band, actin. Numbers below bands indicate protein concentrations in μ M as determined by densitometry. (B) Representative Coomassie-Blue-stained gel showing F-actin binding of coronin 1B at indicated KCl concentrations (1.1 μ M total actin, 1.3 μ M coronin 1B). (C,D) Representative immunoblot showing F-actin bound coronin 1B in the pellets of high-speed co-sedimentation experiments (top panel); Coomassie-Blue-stained gel show the corresponding actin pellets (bottom panel). Identical amounts of coronin 1B (0.1 μ M) were used and concentrations of total ADP- and ATP-G-actin used in each lane are indicated above the blots. In this experiment, the ATP G-actin used was recharged from ADP-G-actin as described previously (Pollard, 1986). (E) Equilibrium binding of coronin 1B to ADP or ATP/ADP- P_i -F-actin filaments. Bound coronin 1B was calculated from the depletion of coronin 1B from the supernatant fraction of experiments similar to those shown in C and D, and quantified by densitometry. Three different protein preparations were used to generate the data points, which are presented as means \pm standard errors of the mean (\pm s.e.m.). (F) Representative Coomassie-Blue-stained gels comparing F-actin-binding capability of wild-type coronin 1B and R30D mutant. (G) Equilibrium binding of wild-type coronin 1B or R30D mutant to ATP/ADP- P_i -F-actin (1.5 μ M F-actin in pellets).

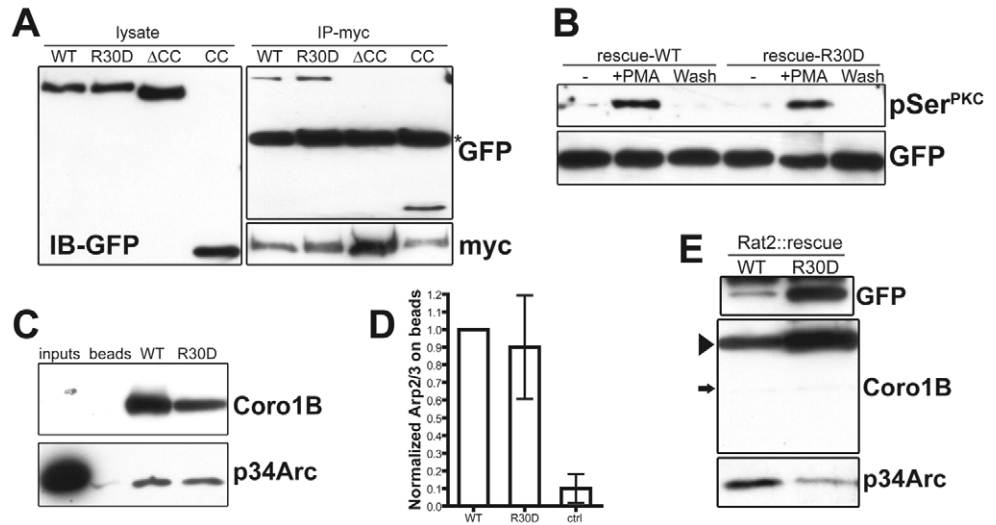
Full-length coronin 1B does not enhance cofilin binding to F-actin

Recent evidence suggests that coronin 1A and cofilin synergize to promote actin depolymerization in an in vitro *Listeria* tail assay (Brierer et al., 2006). To test this observation for coronin 1B, we used a dilution-induced pyrene actin depolymerization assay. We observed that coronin 1B alone cannot induce actin filament depolymerization (Fig. 5A) and coronin 1B protects actin filaments from depolymerization by cofilin (Fig. 5B). Brierer and colleagues showed that coronin 1A enhanced the binding of cofilin to *Listeria* tails and purified actin filaments. To test this mechanism for coronin 1B, we used high-speed actin co-sedimentation assays. In contrast to the previous study, we find that coronin 1B binding to actin filaments is inhibited in

the presence of cofilin, and we see no evidence for enhanced cofilin binding to filaments in the presence of coronin 1B (Fig. 5C). The inhibition of coronin 1B binding by cofilin is reversible by the addition of phalloidin, which blocks the binding of cofilin to actin filaments (Nishida et al., 1987). To test this potential competition more rigorously, we incubated filaments with a constant amount of coronin 1B (1 μ M) and increasing concentrations of cofilin (up to 10 μ M). Increasing cofilin decreased the amount of coronin 1B associated with filaments in a dose-dependent manner (Fig. 5D). In a converse experiment, we incubated filaments with a constant amount of cofilin (1 μ M) and increasing concentrations of coronin 1B (up to 4 μ M). As with the cofilin dose-response experiment, increasing concentrations of coronin 1B decreased the binding of cofilin to actin filaments (Fig. 5E). Similar results were

Fig. 4. The R30D mutation does not perturb other known coronin 1B molecular interactions. (A) HEK293 cells were co-transfected with Myc-tagged coronin 1B and various GFP-tagged coronin 1B mutants: wild type (WT), R30D mutant, coil-coiled domain (CC, 451-489) alone or a deletion mutant lacking the coil-coiled domain (Δ CC, 1-450). We immunoprecipitated Myc-tagged coronin 1B with Myc antibodies and blotted with either anti-GFP or Myc antibodies. The results demonstrate that the coiled-coil domain of coronin 1B is both necessary and sufficient for oligomerization and that the R30D mutation does not affect oligomerization. (B) Rat2 fibroblasts were infected with the knockdown/rescue lentivirus

expressing the coronin 1B shRNA and either wild-type coronin 1B or the R30D mutant. Cells were subjected to the *in vivo* phosphorylation and dephosphorylation assay described in Materials and Methods. (C) *In vitro* direct-binding assay using purified coronin 1B immobilized on Ni-NTA beads and purified bovine Arp2/3 complex in solution (5 nM). (D) Bound Arp2/3 complex on beads from experiments described in C was quantified by densitometry and normalized to the amount of coronin 1B. Results from three independent experiments are presented as the mean \pm s.d. (E) Cells as described in B were lysed and GFP-tagged coronin 1B was immunoprecipitated using anti-GFP antibodies. To visualize the co-immunoprecipitated Arp2/3 complex, the R30D lane was intentionally overloaded. Arrowhead, GFP-tagged coronin 1B; arrow, endogenous coronin 1B.



obtained with recombinant coronin 1A (supplementary material Fig. S7), indicating this competitive binding is not an isoform-specific property. Thus, our results indicate that coronin 1B and cofilin do not synergize directly to promote actin depolymerization and that their binding to actin filaments is antagonistic.

In an effort to reconcile our results with the published results for coronin 1A, we tested a number of coronin 1B mutants in the actin co-sedimentation assay described above. Interestingly, we found that the coronin 1B Δ CC mutant that lacks the coil-coiled domain (Δ CC, 1-450) slightly enhanced the binding of cofilin to actin filaments (Fig. 5F) despite the fact that this mutant lacks high affinity F-actin binding (supplementary material Fig. S9B).

Coronin 1B can bundle F-actin *in vitro*

Since ectopically expressed coronin 1B induces actin cables in S2 cells and yeast coronin is known to bundle actin filaments *in vitro* (Goode et al., 1999), we tested whether coronin 1B can bundle F-actin *in vitro* using two assays. First, we used negative staining and electron microscopy on actin filaments incubated with various concentrations of coronin 1B. Whereas actin filaments alone occasionally have regions that lie in close apposition (inset of Fig. 6A), 10 nM coronin 1B appeared to increase the bundling of actin filaments (Fig. 6B). When coronin 1B (1 μ M) was mixed with an equimolar concentration of F-actin, we observed large actin bundles (Fig. 6C). By contrast, the R30D mutant that lacks F-actin binding does not induce any actin bundles under the same experimental conditions (Fig. 6D). We confirmed this observation by low-speed actin co-sedimentation (Fig. 6E). Since the coronin 1B Δ CC mutant cannot form actin cables in S2 cells (supplementary material Fig. S9A) or actin bundles *in vitro* (data to shown), both coiled-coil-mediated oligomerization and

high-affinity F-actin binding are required for the actin-bundling activity of coronin 1B.

High-affinity F-actin binding is required for stable leading edge localization of coronin 1B

To study the importance of high-affinity F-actin binding for coronin 1B function *in vivo*, we used an established lentiviral knockdown/rescue system to generate cells that express only the R30D mutant, but not endogenous coronin 1B (Cai et al., 2007). Briefly, we identified a short hairpin RNA (shRNA) that specifically depletes rat and mouse coronin 1B (supplementary material Fig. S5A), and co-expressed it along with human coronin 1B tagged with GFP (supplementary material Fig. S5B). Human coronin 1B is refractory to the shRNA because of multiple sequence mismatches. In cells infected with the lentivirus-expressing GFP-tagged coronin 1B, the endogenous protein was efficiently silenced and the GFP-tagged 'rescue' protein was expressed at physiological levels (supplementary material Fig. S5C,D).

To test whether high-affinity actin binding contributes to the localization of coronin 1B to the lamellipodia, we compared wild-type coronin 1B-GFP with the R30D mutant using the knockdown/rescue system in Rat2 fibroblasts. The localization pattern of the Arp2/3 complex (visualized by p34Arc immunostaining), cortactin, F-actin (visualized by phalloidin staining) and VASP were not affected upon expression of either wild-type coronin 1B or the R30D mutant (Fig. 7A,B). The leading edge localization of the R30D mutant was diminished relative to the wild-type protein (Fig. 7B). To quantify the localization differences between these proteins, we performed lamellipodial colocalization analysis across multiple cells (Fig. 7C). An index of leading edge enrichment relative to the cell body was calculated for cells expressing GFP alone, wild-type coronin 1B or the

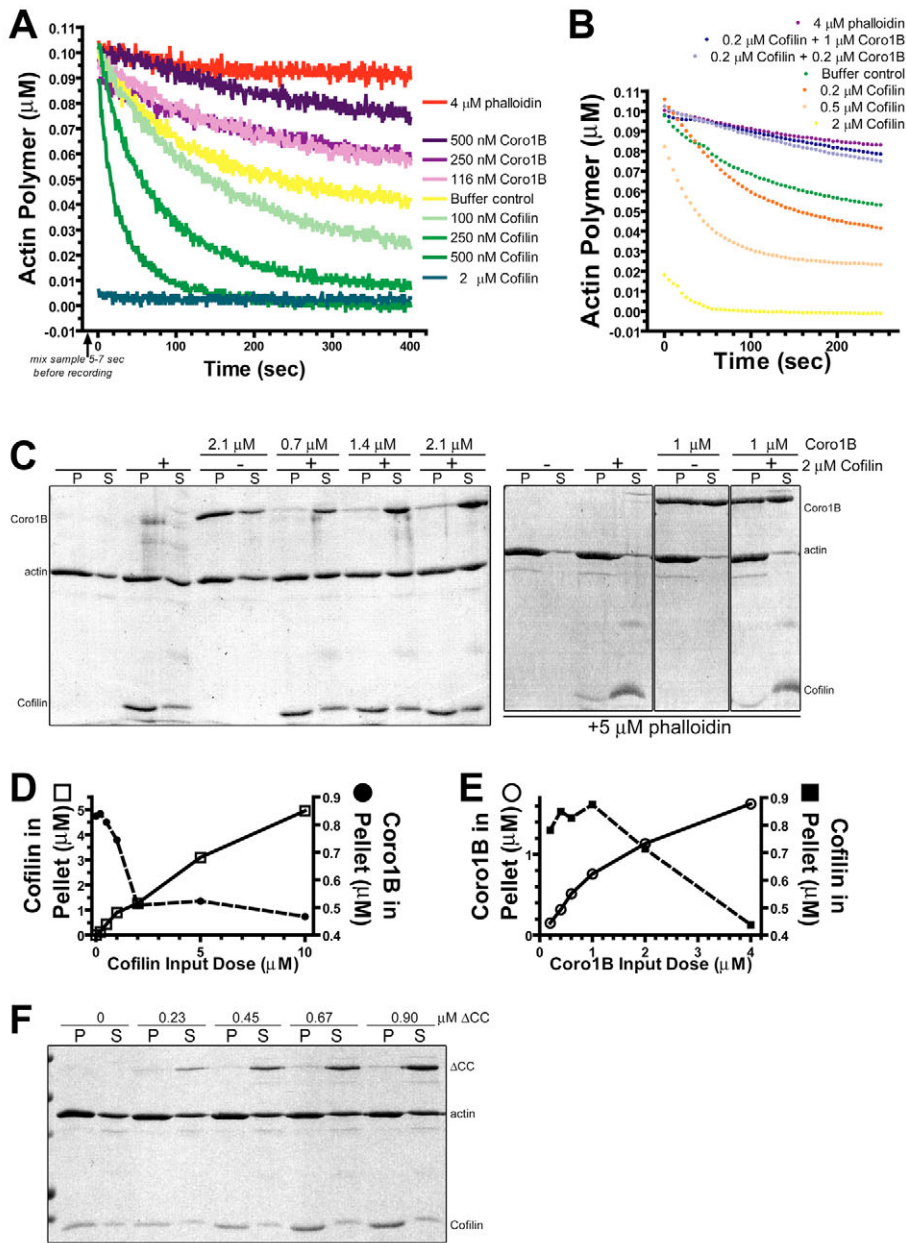


Fig. 5. Coronin 1B protects filaments from cofilin-induced depolymerization and binds antagonistically with cofilin to F-actin. (A) Time course of actin polymer concentration assembled from rabbit smooth muscle ATP G-actin, 30% pyrene labelled, after dilution from 5 μM to 0.1 μM , either alone, with phalloidin or in the presence of coronin 1B and cofilin. (B) Same experimental conditions as in A with phalloidin, coronin 1B and cofilin, or in the presence cofilin alone. (C) Representative Coomassie-Blue-stained gels showing the F-actin binding ability of coronin 1B in the presence of 2 μM cofilin, with or without pre-incubating actin filaments with 5 μM phalloidin. (D) Equilibrium binding of cofilin to actin filaments (assembled from 2 μM ATP G-actin and stored at 4°C overnight) in the presence of 1 μM coronin 1B. (E) Equilibrium binding of coronin 1B to 2 μM actin filaments in the presence of 1 μM cofilin. (F) Representative Coomassie-Blue-stained gel showing the high-speed actin co-sedimentation assay using increasing concentrations of the coronin 1B ΔCC mutant with 2 μM actin and 1 μM cofilin.

R30D mutant. GFP-tagged wild-type coronin 1B has a similar distribution profile to the endogenous protein, whereas the R30D mutant has reduced leading edge enrichment.

Similarly, the coronin 1B ΔCC mutant (which lacks high-affinity F-actin binding) localizes poorly to the leading edge (supplementary material Fig. S9C), despite the fact that this mutant is capable of interacting with the Arp2/3 complex *in vivo* (supplementary material Fig. S9D). Together, these results indicate that, although other coronin 1B interactions may contribute to targeting, F-actin binding is required for normal leading edge localization of coronin 1B.

To test the contribution of F-actin binding to the dynamics of coronin 1B protein, we used fluorescence recovery after photobleaching (FRAP) analysis. In the case of wild-type protein, a spot at the leading edge (Spot1) was compared with a spot in the cytoplasm (Spot2). The leading edge has a slower rate of fluorescence recovery and a larger immobile fraction than the cytoplasm, suggesting that coronin 1B stably interacts with a factor in the lamellipodium (Fig. 7D-G and supplementary material Fig. S8). By contrast, the recovery kinetics of the R30D mutant were identical between the leading edge and the cytoplasm (Fig. 7F,G and supplementary material Fig. S8C), indicating that high-affinity F-actin binding is required for the stable leading edge localization of coronin 1B.

F-actin binding mutants fail to rescue motility phenotypes induced by coronin 1B depletion

To test the requirement of F-actin binding for the function of coronin 1B *in vivo*, we compared the motility of cells expressing either wild-type coronin 1B or the R30D mutant generated using our knockdown/rescue system. We analyzed the whole-cell motility of these cells by single-cell tracking. As observed previously, depletion of coronin 1B in fibroblasts leads to an ~33% decrease in whole-cell speed relative to uninfected control cells, cells infected with a non-specific shRNA (NS) or cells rescued with shRNA-resistant human coronin-1B-GFP fusion protein (Fig. 8A) (Cai et al., 2007). The R30D mutant failed to rescue the defect in whole-cell motility observed in coronin-1B-depleted cells (Fig. 8A). Identical results were obtained with the coronin 1B ΔCC mutant (supplementary material Fig. S9E), indicating that F-actin binding is required for coronin 1B to exert an effect on whole-cell motility *in vivo*. We also employed kymography analysis to examine the

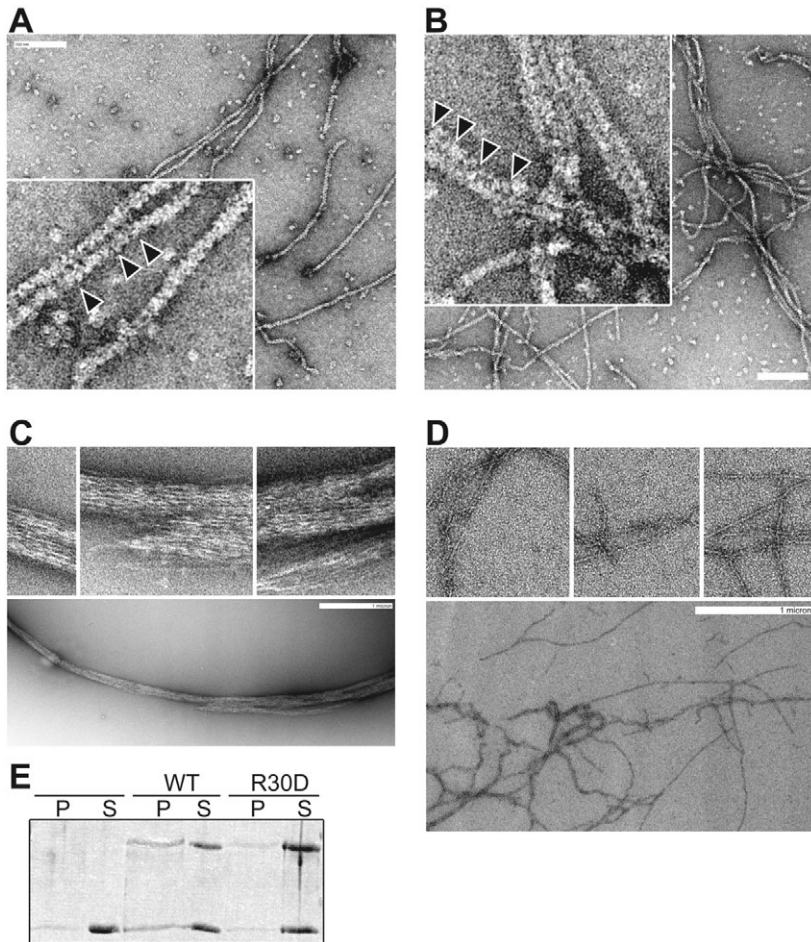


Fig. 6. Coronin 1B can bundle actin filaments in vitro. (A) Electron micrograph of actin filaments, inset showing 4 \times magnification. Actin filaments (1 μ M) were negatively stained and examined by transmission electron microscopy. Arrowheads indicate areas where filaments lie with close apposition; bar, 100 nm. (B) Electron micrograph of actin filaments (1 μ M) with coronin 1B (10 nM); bar, 100 nm. (C,D) Electron micrograph of actin filaments (1 μ M) with either wild-type coronin 1B or the R30D mutant (1 μ M); bar, 1 μ m. (E) Representative Coomassie-Blue-stained gel showing low-speed co-sedimentation of coronin 1B with F-actin. Samples were prepared as described in C and D, then subjected to centrifugation for 5 minutes at 13,000 g .

lamellipodial protrusion dynamics of cells expressing wild-type or R30D coronin 1B. Depletion of coronin 1B leads to increased protrusion rate, reduced protrusion persistence and decreased protrusion distance (Fig. 8B-D). Whereas the wild-type coronin 1B can rescue these defects the R30D mutant cannot, indicating that high-affinity F-actin-binding activity is required for coronin 1B to regulate lamellipodial dynamics at the leading edge. Together, these results demonstrate that the interaction of coronin 1B with F-actin is important for its localization and is essential for in vivo function.

Discussion

Our results support a number of conclusions about the interaction of coronin 1B and F-actin. First, coronin 1B interacts with F-actin via a charged patch on the top surface of its β -propeller domain that contains the highly conserved R30

residue. Second, coronin 1B binds selectively and with high affinity to actin filaments composed of ATP/ADP- P_i subunits. Consistent with this nucleotide preference, coronin 1B and cofilin bind antagonistically to actin filaments. Third, the interaction of coronin 1B with F-actin is responsible for a significant fraction of the lamellipodial enrichment observed with this protein. Fourth, the interaction of coronin 1B with F-actin is absolutely required for its physiological function at the leading edge of motile cells.

Interaction of coronin 1B with F-actin in vitro
Coronins have been known as F-actin binding proteins since their discovery (de Hostos et al., 1991) and the work presented here addresses a number of significant gaps in our understanding of the interaction between coronins and F-actin. Our results indicate that coronin 1B binds preferentially to actin filaments composed of ATP/ADP- P_i subunits with high affinity (170 nM). This preference for ATP/ADP- P_i actin filaments is similar to that of cortactin, another actin-binding protein with an almost identical localization pattern in lamellipodia (Bryce et al., 2005). The actin filaments in lamellipodia are highly dynamic and are thought to be composed mainly of ATP/ADP- P_i subunits. Thus, the preference of coronin 1B to bind ATP/ADP- P_i -F-actin filaments may help to selectively enrich this protein in the lamellipodia over other actin-filament-containing structures such as stress fibers.

Not only does coronin 1B bind to actin filaments, it also bundles these filaments into parallel arrays – as has been observed for other coronins (Goode et al., 1999). Although this effect is seen in vitro and with high-level ectopic expression in *Drosophila* S2 cells, it is unclear whether coronin 1B plays a significant role in bundling actin filaments in mammalian cells. In vitro, strong bundling is only observed when the ratio between coronin 1B and F-actin approaches 1:1. In vivo, the intercellular concentration of coronin 1B is 0.73 μ M (Cai et al., 2007) while the concentration of polymerized actin is estimated to be near 100 μ M (Pollard et al., 2000), suggesting that stoichiometry does not favor coronin 1B-driven bundling in the cytoplasm. Furthermore, unlike proteins such as fascin, coronin 1B is not strongly enriched in bundled F-actin structures, even within the lamellipodium (data not shown). The coiled-coil domain of coronin 1B is required for both bundling and high-affinity F-actin binding in vitro. These results suggest that oligomerization affects bundling as previously shown (Goode et al., 1999), but also increases the apparent affinity of coronin 1B's interaction with filaments. This increased apparent affinity is probably due to effects on avidity, rather than a second F-actin-binding site because the coiled-coil domain displays no detectable F-actin-binding activity on its own (data not shown).

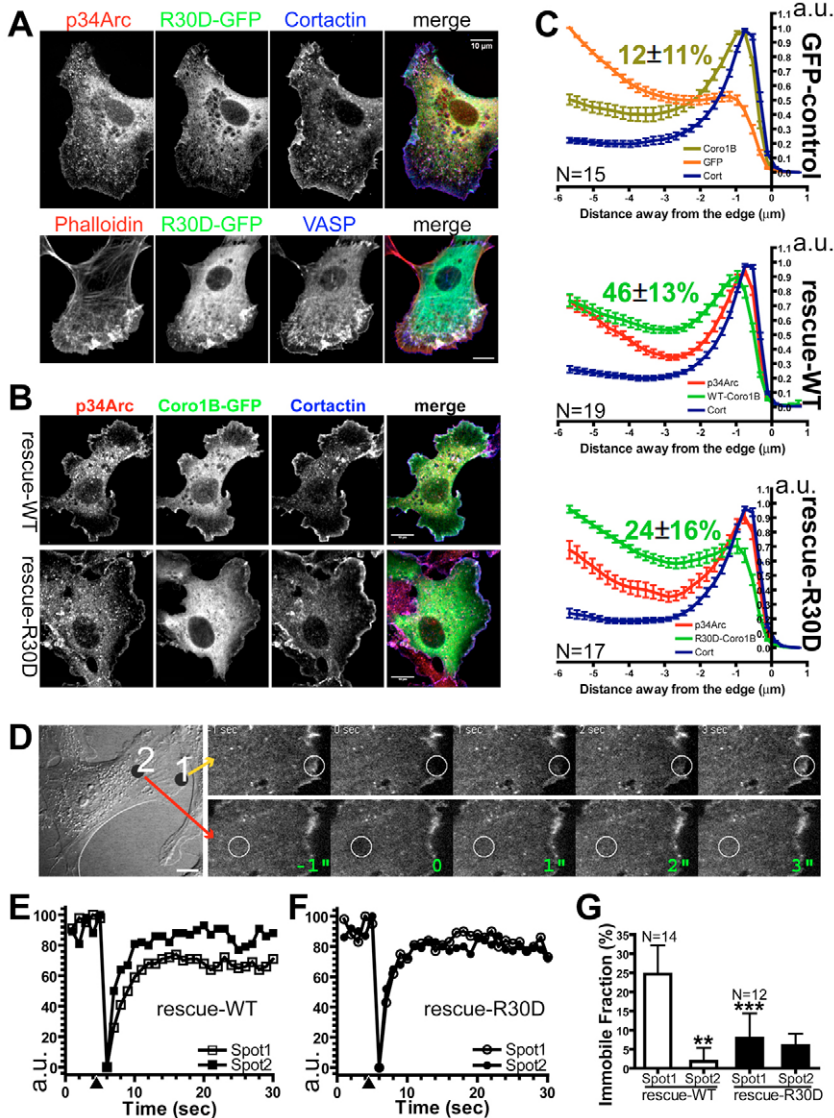


Fig. 7. F-actin binding is required for efficient and stable leading edge localization of coronin 1B. (A) Rat2 fibroblasts expressing GFP-tagged R30D mutant and lacking endogenous coronin 1B were EGF-stimulated (2 minutes) and stained for the Arp2/3 complex (p34Arc subunit), cortactin, F-actin (phalloidin) and VASP. (B) Rat2 fibroblasts lacking endogenous coronin 1B and expressing GFP-tagged wild-type protein (WT) or R30D mutant protein were stained for the Arp2/3 complex (p34Arc subunit) and cortactin following recovery from ATP depletion. (C) The lamellipodial colocalization analysis was performed on the protruding areas of the Rat2 fibroblasts prepared as in B. Fluorescence intensity values were normalized, combined from multiple cells. N, number of cells analyzed per treatment; data are given as the mean \pm s.e.m. (Top) Endogenous coronin 1B, soluble GFP and Cortactin. (Middle and bottom) GFP-tagged coronin 1B (WT or R30D), p34Arc (Arp2/3) and cortactin. The indexes of relative leading edge enrichment of GFP signals from various cells were calculated and presented as the percentile mean \pm s.d. in the center of the graphs. (D) Representative Rat2 fibroblast, whose endogenous coronin 1B was replaced with GFP-tagged wild-type protein, was subjected to fluorescence recovery after photobleaching (FRAP) analysis. A differential interference contrast (DIC) image is presented on the left and individual frames from time-lapse imaging of GFP are presented on the right. Bleached regions are circled; 1, lamellipodia; 2, cytoplasm. (E,F) Representative fluorescent intensity profiles from the two-spot FRAP analysis of Rat2 fibroblasts whose endogenous coronin 1B was replaced with GFP-tagged wild-type protein or GFP-tagged R30D mutant. (G) Statistical analysis of the FRAP immobile fraction across multiple cells. Data are presented as the mean, error bars indicate 95% confidence intervals. Dunnett multiple comparison test was performed as the post-test for one-way ANOVA using the first column as control. N, number of cells analyzed per treatment; ** $P < 0.01$, *** $P < 0.001$.

Several lines of experimental evidence suggest that coronins and ADF/cofilin proteins cooperate to enhance actin depolymerization (Briehner et al., 2006; Cai et al., 2007; Goode et al., 1999), but the precise mechanism of this effect is unclear. Unlike a previous study, we see no evidence for direct enhancement of cofilin binding to F-actin or cofilin-induced depolymerization of filaments by coronins (Briehner et al., 2006). In fact, full-length coronin 1A and 1B bind antagonistically with cofilin to F-actin in co-sedimentation assays. At the moment, the reasons for the discrepancies between these results are unclear. Interestingly, we do observe a slight enhancement of cofilin binding to F-actin in the presence of the coronin 1B Δ CC mutant. Although this result is intriguing, we know of no evidence for regulated oligomerization of coronins or the existence of truncated (monomeric) forms of this protein. Therefore, this result is unlikely to represent a physiologically relevant mechanism for coronin function.

The antagonism between full-length coronin and cofilin for F-actin binding is unlikely to arise from competition for the

same binding site on actin filaments, but rather reflects the binding preferences of coronin 1B for ATP/ADP- P_i -F-actin and cofilin for ADP-F-actin (Blanchoin and Pollard, 1999). Since cofilin enhances the release of inorganic phosphate from actin, it will convert ADP- P_i -F-actin to ADP-F-actin and indirectly inhibit coronin 1B binding (Blanchoin et al., 2000). It will be interesting to test whether coronin 1B inhibits phosphate release from filaments and preserves ADP- P_i -F-actin. Recent data from our lab indicate that coronin 1B targets the cofilin-activating phosphatase slingshot-1L to the leading edge of migrating fibroblasts, suggesting a more indirect mechanism by which coronin and cofilin cooperate in vivo (Cai et al., 2007).

The precise location of the F-actin binding site of coronin is controversial and little consensus exists among the previous studies that addressed this point (Utrecht and Bear, 2006). In this study, we have identified a single, highly conserved arginine residue (R30) on the β -propeller of coronin 1B that is crucial for F-actin binding both in vivo and in vitro. Mutation of this residue does not disrupt coronin 1B structure or interactions with other

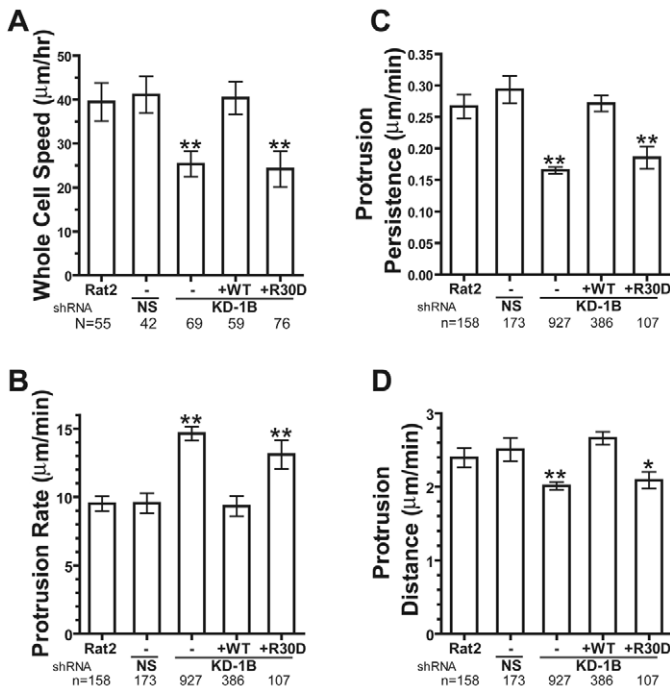


Fig. 8. The R30D mutant cannot rescue depletion phenotypes of coronin 1B. (A) Rat2 fibroblasts were infected with lentivirus expressing coronin 1B shRNA (KD-1B) without or with GFP-tagged wild-type or GFP-tagged R30D coronin 1B or with control shRNA (NS). Cells were subjected to single-cell tracking. Data are presented as mean cell speed, error bars indicate 95% confidence intervals. (N, number of cells tracked per treatment; ** $P < 0.01$). (B–D) Cells described in A were subjected to kymography analysis. Protrusion parameters were determined from at least six randomly selected cells; n, number of protrusion events analyzed per treatment. Data are presented as the mean, error bars indicate 95% confidence intervals. Dunnett multiple comparison test was performed as a post-test for one-way ANOVA using the first column as control; * $P < 0.05$, ** $P < 0.01$.

molecular partners, indicating that this mutation selectively affects F-actin binding. The fact that the R30 residue is on the top surface of the β -propeller is not surprising because this is a common location for binding interfaces on proteins of this type and previous structural studies of coronin 1A postulated a potential binding surface containing this residue (Appleton et al., 2006). Future studies will test whether F-actin interacts with other residues in this patch.

The role of interactions between coronin 1B and F-actin in vivo

One logical assumption about the coronin family of proteins is that they must interact with F-actin in order to localize properly and/or exert their biological effects. With the R30D mutant of coronin 1B in hand, we were able to formally test this notion. The R30D mutant shows reduced localization to the leading edge of fibroblasts relative to the wild-type protein, but does show some enrichment relative to soluble GFP. This suggests that other coronin 1B interactions such as Arp2/3 binding may drive some localization to the lamellipodium. Alternately, the residual F-actin-binding activity of the R30D mutant may be sufficient to provide some leading edge targeting. Regardless

of the precise mechanism of the weak R30D localization, our FRAP analysis indicates that high-affinity F-actin binding is required for stable localization of coronin 1B to the leading edge.

Coronin 1B coordinates Arp2/3 complex and cofilin activities (via slingshot-1L) in the lamellipodium of migrating fibroblasts (Cai et al., 2007). Upon coronin 1B depletion, whole-cell motility is reduced and lamellipodial dynamics are altered. These phenotypes arise from defects in the dynamics and organization of actin filaments at the leading edge. The results presented here indicate that F-actin binding is absolutely required for coronin 1B to exert its effects on motility. These data have important implications for the mechanism of coronin 1B function. For example, coronin function must include an obligate F-actin-binding step. The R30D mutant described in this work will be an invaluable tool for dissecting the mechanism of coronin function in future studies.

Materials and Methods

Materials

Commercial antibodies were obtained from Cell Signaling Technologies (pSer^{PKC}), Upstate Biotechnology (p34Arc, 4F11/Cortactin), Roche (7.1+13.1/GFP), Sigma (9E10/myc), Santa Cruz (yN16/Arp2) and Jackson ImmunoResearch (Rhodamine Red-X, Cy5, and horseradish-peroxidase-conjugated secondary antibodies). Alexa Fluor dyes conjugated to phalloidin were from Molecular Probes. Inhibitors Ro32-0432 and okadaic acid were from Calbiochem. Protease and phosphatase inhibitors (phenylmethylsulfonyl fluoride, 1,10-phenanthroline, aprotinin, leupeptin, sodium fluoride and sodium orthovanadate) were from Sigma. All other materials were from Fisher Scientific unless otherwise indicated. Rabbit muscle G-actin and bovine Arp2/3 complex were generous gifts from Dorothy Schafer (University of Virginia, Charlottesville, VA).

Cell culture and viral transduction

Mammalian cell culture, immunoprecipitation and immunoblotting were performed as previously described (Bear et al., 2000; Cai et al., 2005). Transient transfections were performed using FuGENE 6 (Roche) for HEK293 cells according to the manufacturer's protocol. Lentivirus production and infection were performed as described previously (Rubinson et al., 2003).

Molecular cloning

PCR and subcloning were performed using standard methods. Detailed methods and primer sequences are available upon request. Plasmids expressing wild-type coronin 1B were constructed as previously described (Cai et al., 2005). Coronin 1B–coronin-2A chimeras and mutations on coronin 1B were generated by overlapping PCR and verified by sequencing. *Drosophila* S2 cell expression constructs were generated by sub-cloning coronin 1B-EGFP fragments into the pAc5.1/V5-HisA vector (Invitrogen). For mammalian cell protein expression, the coronin 1B coding sequence was inserted into the multi-cloning sites of the pTT5SH8Q2 vector that contains the StrepTagII and 8xHis affinity tags (Durocher et al., 2002; Shi et al., 2005). The lentiviral knockdown constructs used have been described previously (Cai et al., 2007).

Drosophila S2 cell actin-cable-formation assay

Drosophila S2 cells were cultured as previously described with slight modifications (Rogers et al., 2003). Briefly, S2 cells were maintained in Schneider's *Drosophila* medium (Gibco) supplemented with 10% heat-inactivated FBS (HyClone), 100 units/ml penicillin, 100 μ g/ml streptomycin and 292 μ g/ml glutamine (Gibco). S2 cells were transfected using CellFectin reagent (Invitrogen) according to the manufacturer's protocol. For high-resolution imaging, S2 cells were plated on concanavalin A (ConA)-coated coverslips and stained according to standard protocols.

Silencing of endogenous *Drosophila* p20Arc was performed as previously described (Rogers et al., 2003). Briefly, depletion by RNA interference (RNAi) was performed on S2 cells for 7 days according to methods previously published (Clemens et al., 2000), using PCR products flanked at their 5' and 3' ends by T7 sequences (p20Arc primers: 5'-CAGACAACAACCCGACACC-3' and 5'-CAGT-TTCATTTCGCTGATCTCC-3'). On day 5, p20Arc-depleted cells were transfected with the coronin 1B expression construct.

Production of recombinant coronin 1B protein

Recombinant coronin 1B protein was expressed and purified from a mammalian expression system as described previously (Cai et al., 2007).

Actin co-sedimentation

High-speed actin co-sedimentation was performed, with modifications, as previously described (Bryce et al., 2005). Briefly, F-actin was prepared from actin monomers by polymerization in the presence of 50 mM KCl, 2 mM MgCl₂, 5 mM Tris-Cl pH 8.0 and 1 mM ATP for 30 minutes at room temperature. Coronin 1B was incubated with F-actin at room temperature for 1 hour (with 4% glycerol), and sedimented using an Airfuge (Beckman) at 23 psi (~100,000 g) for 30 minutes. Pellet and supernatant samples were prepared for SDS-PAGE using standard procedures. To calculate the binding affinity (K_d) of coronin 1B to F-actin, we used an established supernatant-depletion method (Bryce et al., 2005). Coronin 1B bound to F-actin ($[1B_p]$) was determined indirectly by immunoblotting the supernatant and quantified by densitometry: $[1B_s]=0.1 \mu\text{M}$. All blots were within the linear range of detection (data not shown). F-actin concentrations $[Fa]$ were calculated from total G-actin concentration and the known critical concentrations for ATP-G-actin (0.1 μM) and ADP-G-actin (5 μM). ADP-G-actin was prepared as previously described and used within 4 hours (Pollard, 1986). In order to appropriately compare ADP- with ATP-F-actin, the ATP-G-actin used for affinity measurements (Fig. 3C,D) was regenerated from ADP-G-actin by diluting the stock of ADP-G-actin from 20 μM to 5 μM with 0.1 mM MgCl₂, 0.1 mM EGTA pH 8.0 and 1 mM ATP. To calculate the F-actin-binding affinity of coronin 1B, the following equation was used to fit the experimental data:

$$[1B_p] = \frac{K_d + [1B_s] + [Fa] - \sqrt{(K_d + [1B_s] + [Fa])^2 - 4[1B_s][Fa]}}{2} \quad (1)$$

Statistical analysis and graphing were performed with Prism (GraphPad).

Low-speed actin co-sedimentation was performed as previously described (Goode et al., 1999). Briefly, 1 μM coronin 1B was mixed with 1 μM ATP F-actin and incubated for 2 hours at room temperature. The reactions were subjected to centrifugation at low speed (13,000 g) for 5 minutes, and pellet and supernatant samples were analyzed as described above.

Pyrene-actin depolymerization assay

Pyrene-actin depolymerization assay was performed as previously described (Moseley et al., 2006). Briefly, 5 μl of 5 μM ATP-G-actin (30% pyrene labeled) was polymerized at room temperature for 1 hour in F-buffer (10 mM Tris-HCl pH 7.5, 0.2 mM DTT, 0.2 mM CaCl₂, 50 mM KCl, 2 mM MgCl₂, and 0.7 mM ATP), with or without 5 μM phalloidin (final concentration). To initiate depolymerization, 245 μl MKEL-50 buffer (20 mM imidazole pH 7.0, 50 mM KCl, 2 mM MgCl₂, 1 mM EGTA, 0.5 mM DTT) was added to the 5 μl pre-assembled actin filaments (final concentration 0.1 μM actin in reaction) with or without coronin 1B and/or cofilin. His-tagged cofilin was purified by standard methods. Care was taken to avoid filament shearing. Pyrene fluorescence was monitored at 25°C (Fig. 5A, 1-second interval; Fig. 5B, 5-second interval; excitation 365 nm, emission 386 nm). Fluorescence was converted to the molar concentration of F-actin from the initial fluorescence of phalloidin-stabilized actin (assuming to be all F-actin) and the final fluorescence of 2 μM cofilin treated sample (assuming to be all G-actin).

Partial proteolysis and circular dichroism analysis

For partial proteolysis reactions, 6 μg of wild-type coronin or R30D mutant protein was mixed with 20 ng protease K and incubated at 55°C. Reactions were stopped at fixed time points by mixing with 2 \times SDS sample buffer and by immediate boiling of the sample. Samples were separated by PAGE and visualized by silver staining. To perform circular-dichroism analysis, protein samples were dialyzed in 5 mM pH 7.4 Na₂HPO₄/NaH₂PO₄ buffer overnight at 4°C. Circular-dichroism spectra were obtained using a Pistar-180 Circular Dichroism/Fluorescence spectrometer (Applied Photophysics), scanning from 260-185 nm at 0.2-nm steps.

In vivo coronin 1B dephosphorylation assay

Coronin 1B phosphorylation/dephosphorylation assays were performed as described (Cai et al., 2007).

Light microscopy and image analysis

Immunofluorescent staining and imaging were performed as previously described (Cai et al., 2005). Except where indicated, cells were imaged using spinning disk confocal microscopy. To stimulate uniform lamellipodial protrusion, Rat2 cells were treated with sodium azide (PBS supplemented with 0.1 g/l CaCl₂, 0.1 g/l MgCl₂, and 20 mM NaN₃) for 30 minutes, and recovered with fresh culture media for 5 minutes before fixation. Lamellipodial colocalization analysis was performed as described previously (Cai et al., 2007). Pixel intensity information from $-3 \mu\text{m}$ to $0 \mu\text{m}$ was used to generate an index of relative leading edge enrichment. This index was calculated using the equation $[(L-C)/L]$ where L is the lamellipodial peak intensity, and C is cell body minimum intensity and presented as percentile score.

Fluorescence recovery after photobleaching (FRAP) movies were captured using a FluoView FV1000 scanning confocal microscope (Olympus) equipped with a 405 nm laser and a 60 \times objective (N.A. 1.4). Photobleaching was performed using

tornado mode for 100 milliseconds on a circular area (28-pixel diameter). Fluorescence intensities from the bleached area were measured using ImageJ, and analyzed and graphed in Prism. The fluorescence intensities before irradiation and 20 seconds after photobleaching were used to calculate the FRAP immobile fractions.

Transmission electron microscopy

An equal volume of either 20 nM or 2 μM coronin 1B was mixed with F-actin (2 μM Mg-ATP G-actin, pre-assembled for 30 minutes) and incubated for 1 hour at room temperature. Aliquots of these samples were adsorbed directly onto glow-charged thin carbon foils on 400-mesh copper grids without fixation and stained with 2% (w/v) uranyl acetate. The grids were examined in a Philips CM12 microscope at 80 kV. The images were taken at magnification 10,000 \times or 45,000 \times on Kodak SO-163 film, scanned using an Imacon FlexTight 848 scanner (Hasselblad AB) at resolution 2500 dpi and adjusted for publication using Photoshop (Adobe).

Single-cell tracking and kymography analysis

Single-cell tracking and kymography assays and analysis were performed as described previously (Cai et al., 2007).

We gratefully acknowledge Eric Vitriol for help with FRAP microscopy; Andrea Uetrecht and Steve Rogers for RNAi in *Drosophila* S2 cells; Ken Jacobson for helpful discussions about FRAP analysis; Hao Wu, Steve Rogers, David Roadcap for critical reading of the manuscript; Dorothy Schafer for reagents and assistance with the pyrene actin depolymerization assay; Yves Durocher and Keith Burridge for reagents. Circular dichroism measurement was performed at Macromolecular Interaction Facility in UNC, with the help from Ashutosh Tripathy. Electron microscopy work was supported by NIH grant CA-16086 to Jack D. Griffith (UNC). This work was supported by funds from Carolina Center for Cancer Nanotechnology Excellence (NCI; 1U54CA119343) and the Sontag Foundation.

References

- Appleton, B. A., Wu, P. and Wiesmann, C. (2006). The crystal structure of murine coronin-1: a regulator of actin cytoskeletal dynamics in lymphocytes. *Structure* **14**, 87-96.
- Bamburg, J. R. (1999). Proteins of the ADF/cofilin family: essential regulators of actin dynamics. *Annu. Rev. Cell Dev. Biol.* **15**, 185-230.
- Bear, J. E., Loureiro, J. J., Libova, I., Fassler, R., Wehland, J. and Gertler, F. B. (2000). Negative regulation of fibroblast motility by Ena/VASP proteins. *Cell* **101**, 717-728.
- Bear, J. E., Krause, M. and Gertler, F. B. (2001). Regulating cellular actin assembly. *Curr. Opin. Cell Biol.* **13**, 158-166.
- Blanchoin, L. and Pollard, T. D. (1999). Mechanism of interaction of Acanthamoeba actophorin (ADF/cofilin) with actin filaments. *J. Biol. Chem.* **274**, 15538-15546.
- Blanchoin, L., Pollard, T. D. and Mullins, R. D. (2000). Interactions of ADF/cofilin, Arp2/3 complex, capping protein and profilin in remodeling of branched actin filament networks. *Curr. Biol.* **10**, 1273-1282.
- Briehner, W. M., Kueh, H. Y., Ballif, B. A. and Mitchison, T. J. (2006). Rapid actin monomer-insensitive depolymerization of *Listeria* actin comet tails by cofilin, coronin, and Aip1. *J. Cell Biol.* **175**, 315-324.
- Bryce, N. S., Clark, E. S., Leysath, J. L., Currie, J. D., Webb, D. J. and Weaver, A. M. (2005). Cortactin promotes cell motility by enhancing lamellipodial persistence. *Curr. Biol.* **15**, 1276-1285.
- Cai, L., Holowekyj, N., Schaller, M. D. and Bear, J. E. (2005). Phosphorylation of coronin 1B by protein kinase C regulates interaction with Arp2/3 and cell motility. *J. Biol. Chem.* **280**, 31913-31923.
- Cai, L., Marshall, T. W., Uetrecht, A. C., Schafer, D. A. and Bear, J. E. (2007). Coronin 1B coordinates Arp2/3 complex and cofilin activities at the leading edge. *Cell* **128**, 915-929.
- Clemens, J. C., Worby, C. A., Simonson-Leff, N., Muda, M., Machama, T., Hemmings, B. A. and Dixon, J. E. (2000). Use of double-stranded RNA interference in *Drosophila* cell lines to dissect signal transduction pathways. *Proc. Natl. Acad. Sci. U.S.A.* **97**, 6499-6503.
- de Hostos, E. L., Bradtke, B., Lottspeich, F., Guggenheim, R. and Gerisch, G. (1991). Coronin, an actin binding protein of *Dictyostelium discoideum* localized to cell surface projections, has sequence similarities to G protein beta subunits. *EMBO J.* **10**, 4097-4104.
- de Hostos, E. L., Rehfuess, C., Bradtke, B., Waddell, D. R., Albrecht, R., Murphy, J. and Gerisch, G. (1993). *Dictyostelium* mutants lacking the cytoskeletal protein coronin are defective in cytokinesis and cell motility. *J. Cell Biol.* **120**, 163-173.
- Di Giovanni, S., De Biase, A., Yakovlev, A., Finn, T., Beers, J., Hoffman, E. P. and Faden, A. I. (2005). In vivo and in vitro characterization of novel neuronal plasticity factors identified following spinal cord injury. *J. Biol. Chem.* **280**, 2084-2091.
- Durocher, Y., Perret, S. and Kamen, A. (2002). High-level and high-throughput

- recombinant protein production by transient transfection of suspension-growing human 293-EBNA1 cells. *Nucleic Acids Res.* **30**, E9.
- Engqvist-Goldstein, A. E. and Drubin, D. G.** (2003). Actin assembly and endocytosis: from yeast to mammals. *Annu. Rev. Cell Dev. Biol.* **19**, 287-332.
- Foger, N., Rangell, L., Danilenko, D. M. and Chan, A. C.** (2006). Requirement for coronin 1 in T lymphocyte trafficking and cellular homeostasis. *Science* **313**, 839-842.
- Gatfield, J., Albrecht, I., Zanolari, B., Steinmetz, M. O. and Pieters, J.** (2005). Association of the Leukocyte Plasma Membrane with the Actin Cytoskeleton through Coiled Coil-mediated Trimeric Coronin 1 Molecules. *Mol. Biol. Cell* **16**, 2786-2798.
- Goode, B. L., Wong, J. J., Butty, A. C., Peter, M., McCormack, A. L., Yates, J. R., Drubin, D. G. and Barnes, G.** (1999). Coronin promotes the rapid assembly and cross-linking of actin filaments and may link the actin and microtubule cytoskeletons in yeast. *J. Cell Biol.* **144**, 83-98.
- Humphries, C. L., Balcer, H. I., D'Agostino, J. L., Winsor, B., Drubin, D. G., Barnes, G., Andrews, B. J. and Goode, B. L.** (2002). Direct regulation of Arp2/3 complex activity and function by the actin binding protein coronin. *J. Cell Biol.* **159**, 993-1004.
- Liu, C. Z., Chen, Y. and Sui, S. F.** (2006). The identification of a new actin-binding region in p57. *Cell Res.* **16**, 106-112.
- Maniak, M., Rauchenberger, R., Albrecht, R., Murphy, J. and Gerisch, G.** (1995). Coronin involved in phagocytosis: dynamics of particle-induced relocalization visualized by a green fluorescent protein Tag. *Cell* **83**, 915-924.
- Mishima, M. and Nishida, E.** (1999). Coronin localizes to leading edges and is involved in cell spreading and lamellipodium extension in vertebrate cells. *J. Cell Sci.* **112**, 2833-2842.
- Moseley, J. B., Okada, K., Balcer, H. I., Kovar, D. R., Pollard, T. D. and Goode, B. L.** (2006). Twinfilin is an actin-filament-severing protein and promotes rapid turnover of actin structures in vivo. *J. Cell Sci.* **119**, 1547-1557.
- Nishida, E., Iida, K., Yonezawa, N., Koyasu, S., Yahara, I. and Sakai, H.** (1987). Cofilin is a component of intranuclear and cytoplasmic actin rods induced in cultured cells. *Proc. Natl. Acad. Sci USA* **84**, 5262-5266.
- Oku, T., Itoh, S., Okano, M., Suzuki, A., Suzuki, K., Nakajin, S., Tsuji, T., Nauseef, W. M. and Toyoshima, S.** (2003). Two Regions Responsible for the Actin Binding of p57, a Mammalian Coronin Family Actin-Binding Protein. *Biol. Pharm. Bull.* **26**, 409-416.
- Pollard, T. D.** (1986). Rate constants for the reactions of ATP- and ADP-actin with the ends of actin filaments. *J. Cell Biol.* **103**, 2747-2754.
- Pollard, T. D. and Borisy, G. G.** (2003). Cellular motility driven by assembly and disassembly of actin filaments. *Cell* **112**, 453-465.
- Pollard, T. D., Blanchoin, L. and Mullins, R. D.** (2000). Molecular mechanisms controlling actin filament dynamics in nonmuscle cells. *Annu. Rev. Biophys. Biomol. Struct.* **29**, 545-576.
- Rogers, S. L., Wiedemann, U., Stuurman, N. and Vale, R. D.** (2003). Molecular requirements for actin-based lamella formation in Drosophila S2 cells. *J. Cell Biol.* **162**, 1079-1088.
- Rubinson, D. A., Dillon, C. P., Kwiatkowski, A. V., Sievers, C., Yang, L., Kopinja, J., Rooney, D. L., Ihrig, M. M., McManus, M. T., Gertler, F. B. et al.** (2003). A lentivirus-based system to functionally silence genes in primary mammalian cells, stem cells and transgenic mice by RNA interference. *Nat. Genet.* **33**, 401-406.
- Shi, C., Shin, Y. O., Hanson, J., Cass, B., Loewen, M. C. and Durocher, Y.** (2005). Purification and characterization of a recombinant G-protein-coupled receptor, *Saccharomyces cerevisiae* Ste2p, transiently expressed in HEK293 EBNA1 cells. *Biochemistry* **44**, 15705-15714.
- Spoerl, Z., Stumpf, M., Noegel, A. A. and Hasse, A.** (2002). Oligomerization, F-actin interaction, and membrane association of the ubiquitous mammalian coronin 3 are mediated by its carboxyl terminus. *J. Biol. Chem.* **277**, 48858-48867.
- Uetrecht, A. C. and Bear, J. E.** (2006). Coronins: the return of the crown. *Trends Cell Biol.* **16**, 421-426.